

## FREE OVERFALL IN CHANNELS WITH DIFFERENT CROSS SECTIONS AND SUB-CRITICAL FLOW\*

M. K. BEIRAMI,\*\* S. V. NABAVI, AND M. R. CHAMANI

Dept. of Civil Engineering, Isfahan University of Technology, Isfahan, I. R. of Iran  
Email: beirami@cc.iut.ac.ir

**Abstract**– In this paper, based on the free vortex theorem and the momentum equation, a theoretical model to predict the pressure head distribution, the pressure coefficient, the end depth ratio (EDR), and flow discharge at the brink of free overfalls in channels of different cross sections with sub-critical flow is presented. Using available experimental and theoretical results of other investigators for rectangular, triangular, exponential, trapezoidal, inverted triangular ( $\Delta$ -shaped), inverted semicircular and also circular channels, the proposed method has been examined. The presented theory agrees well with the experiments.

**Keywords**– Free overfall, brink depth, drop, end depth ratio, flow measurement

### 1. INTRODUCTION

If the flow at an abrupt end of a long channel is not submerged by the tailwater, it can be referred to as a free overfall. In channels with mild slopes, the approaching flow is sub-critical (Fig. 1). At the upstream control section with a critical depth  $y_c$ , vertical accelerations are negligible and a hydrostatic pressure distribution can be safely assumed. At the brink section with depth  $y_b$ , the pressure distribution is no longer hydrostatic, both due to the curvature of the flow and the aeration of the under nappe. Since there is a unique relationship between the critical depth and flow discharge, the ratio of the end-depth to the critical depth (EDR) offers a possibility to predict the flow discharge and study erosion at the brink of a free overfall. For steep slopes, where the approaching flow is super-critical, flow discharge is a function of end-depth, channel slope, and channel roughness.

Fundamental experimental research was carried out by Rouse to estimate the end depth ratio (EDR), which was found to be 0.715 in mildly sloping confined rectangular channels [1]. Since then, numerous experiments have been conducted to estimate the EDR in channels with various shapes. Recently, Dey did a literature review of these investigations [2]. Other researchers have conducted a large number of experiments and given different theoretical approaches for a single or a few number of channels [3-21].

In this paper, a general theoretical model to predict the EDR and flow discharge in channels of different shapes with approaching sub-critical flow is presented. The proposed model is compared with the existing data and the theoretical approaches from the other researchers outlined above.

### 2. PROPOSED MODEL

Figure 1 shows a free overfall in a prismatic channel of constant bottom slope  $S_0$ . At the end section, the approximate centrifugal pressure head at any streamtube can be computed by Newton's law of

---

\*Received by the editors January 12, 2005; final revised form December 20, 2005.

\*\*Corresponding author

acceleration as  $y_i u_i^2 / (r_i g)$  [22]. Therefore, the pressure head at any streamtube ( $h_i$ ) can be estimated as

$$h_i = y_i \left( 1 - \frac{u_i^2}{r_i g} \right) \tag{1}$$

where  $g$  = acceleration of gravity;  $y_i$ ,  $u_i$  and  $r_i$  are flow depth, flow velocity and radius of curvature of streamtube  $i$ , respectively. The pressure head at the channel bottom of  $b$ - $b$  section is

$$h_B = y_B \left( 1 - \frac{u_B^2}{r_B g} \right) \tag{2}$$

where  $u_B$  and  $r_B$  are the flow velocity and the radius of curvature at the channel bottom of the end-depth. Since  $h_B$  is equal to zero, the radius of streamline curvature at the channel bottom ( $r_B$ ) can be obtained as  $u_B^2 / g$ .

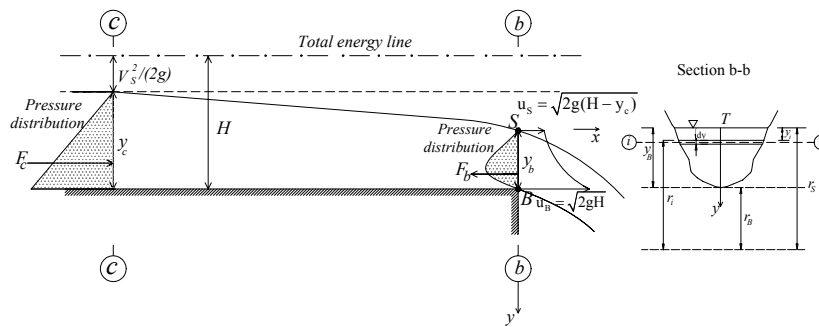


Fig. 1. Definition sketch

The same as Ali and Sykes [9], applying the Bernoulli's theorem to the top (index S) and bottom (index B) streamlines in the brink section, the boundary velocities can be estimated as

$$u_S = \sqrt{2g(H - y_c)} \tag{3}$$

$$u_B = \sqrt{2gH} \tag{4}$$

where  $y_c$  = critical depth at section  $c$ - $c$ ,  $H = y_c + \alpha V_c^2 / (2g) = y_c + D_c / 2$  is specific energy at section  $c$ - $c$ ,  $D = A / T$  is hydraulic depth,  $A$  = flow area,  $T$  = top width of flow,  $\alpha$  = energy correction coefficient which is assumed to be unity. Equation (4) gives  $r_B = 2H$ . Using free-vortex theorem as  $u_i r_i = u_B r_B = C$ , the radius of curvature at any point of section  $b$ - $b$  can be found as

$$r_i = \frac{2H \sqrt{2gH}}{\sqrt{2g[H - y_c + (y_i / y_b) y_c]}} \tag{5}$$

If  $y_b$  is divided into  $n$  parallel streamlines, then for each streamline, Eq. (1) gives the pressure head as

$$h_i = y_i - \frac{y_i [H - y_c + (y_i / y_b) y_c]^{3/2}}{H^{3/2}} \tag{6}$$

In a general case, if  $y = y_i$ , as shown in Fig. 1, the pressure force at the end section is equal to

$$F_b = \gamma \int_0^{y_b} \left\{ y - \frac{y [H - y_c + (y / y_b) y_c]^{3/2}}{H^{3/2}} \right\} dy \tag{7}$$

The above procedure gives the coefficient of pressure distribution as

$$K = F_b / (0.5\gamma y_b^2) \quad (8)$$

Applying the momentum equation to the control volume between sections c-c and b-b in Fig. 1, yields

$$F_c - F_b - \int \tau dx + W \sin \theta = \rho Q (\beta_b V_b - \beta_c V_c) \quad (9)$$

where  $\gamma$ = specific weight of fluid,  $F$ = hydrostatic load,  $\tau$ = wall and bed shear stresses,  $W$ = gravity force of fluid in the control volume,  $\rho$ = mass density of fluid,  $Q$ = flow discharge,  $V$ = mean flow velocity, and  $\beta$ = Boussinesq coefficient, and subscripts c and b refer to sections c-c and b-b, respectively. For simplicity, in this analysis,  $\beta$  is assumed to be unity.

For analytical simplicity, a state of pseudo-uniform flow is assumed within the control volume, where wall and shear stresses are compensated by the stream-wise component of gravity force of fluid. In sub-critical flows, an error of about 1% in estimation of the EDR due to the exclusion of wall and bed shear stresses is obtained [23]. Rajaratnam and Muralindhar [7] have shown that this error is about 3% in horizontal and mildly sloping channels. However, in sub-critical flow for low flow rates, the distance between sections c-c and b-b is of the order of (3~4) yc [22, 23], and as such is sufficiently small for this assumption to be accurate for a first order approximation. Using the above assumptions, Eq. (9) can be simplified as

$$F_c - F_b = \rho Q (V_b - V_c) \quad (10)$$

Introducing  $F_c = \gamma(A \bar{y})_c$  and  $F_b = \gamma K(A \bar{y})_b$  in Eq. (10), one gets

$$\gamma(A \bar{y})_c - \gamma K(A \bar{y})_b = \rho Q (V_b - V_c) \quad (11)$$

where  $\bar{y}$  = depth of the centroid of a cross section below the flow surface. Using  $V=Q/A$  and  $\gamma=\rho g$ , Eq. (11) can be simplified as

$$(A \bar{y})_c - K(A \bar{y})_b = [Q^2 / g][1 / A_b - 1 / A_c] \quad (12)$$

In the critical section, the flow discharge can be computed as

$$Q^2 / g = A_c^3 / T_c \quad (13)$$

Substituting  $Q$  from Eq. (13) into Eq. (12), one gets

$$(A \bar{y})_c - K(A \bar{y})_b = [A_c^2 / T_c][A_c / A_b - 1] \quad (14)$$

Table 1 shows the calculated values of  $A$ ,  $\bar{y}$ ,  $T$  and  $K$  of different channels. In this table,  $b$ = bottom width of rectangular or trapezoidal channel,  $d$  = channel diameter,  $m$ = side slope of trapezoidal or triangular channel,  $N = m/y/b$ ,  $z$  = height of the inverted triangular channel,  $c_1$  and  $c_2$  = constant coefficients which define the channel shape, (e. g., in rectangular channels  $c_1=b$ ,  $c_2=0$  and in triangular channels  $c_1 = 2m$ ,  $c_2 = 1$ ), and  $\hat{y} = y/d$  in circular channels or  $\hat{y} = y/z$  in inverted triangular channels.  $\psi(\hat{y})$  and  $\eta(\hat{y})$  are defined [16, 20] as

$$\psi(\hat{y}) = \arcsin(2\hat{y}) + 2\hat{y}(1-4\hat{y}^2)^{0.5} \quad (15)$$

$$\eta(\hat{y}) = \arccos(1-2\hat{y}) - 2(1-2\hat{y})[\hat{y}(1-\hat{y})]^{0.5} \quad (16)$$

Using Eqs. (14) and (13), the EDR, and consequently, the flow discharge of various channel shapes have been computed. The results for rectangular, triangular and exponential channels are presented in Table 2.

In this table, the possible differences of results between the experiments and the proposed model are also presented.

The presented method can be used for the super-critical flow. In this case, using Manning's equation and a control volume between the brink and uniform flow sections, flow discharges as a function of the end-depth and channel slope can be estimated.

Table 1. Geometric parameters and pressure coefficient for various channels

Cross-Section	A	$\bar{y}$	T	K	
Rectangular	by	y/2	b	0.3033	
Triangular	my <sup>2</sup>	y/3	2my	0.3558	
Exponential	$\frac{c_1}{1+c_2} y^{1+c_2}$	$\frac{y}{2+c_2}$	$c_1 y^{c_2}$	0.3366	
Trapezoidal	by(1+N)	$\frac{2N+3}{6(1+N)} y$	b(1+2N)	$N_c=0$	$N_c=\infty$
				0.3033	0.3558
Inverted triangular	$\frac{(2-\hat{y})\hat{y}}{\sqrt{3}} z^2$	$\frac{3\hat{y}-\hat{y}^2}{6-3\hat{y}} z$	$\frac{2(1-\hat{y})}{\sqrt{3}} z$	$\hat{y}_c \approx 0$	$\hat{y}_c = 1$
				0.3033	0
Inverted semicircular	0.25d <sup>2</sup> $\psi(\hat{y})$	$[\hat{y} - \frac{1-(1-4\hat{y}^2)^{1.5}}{3\psi(\hat{y})}] d$	d(1-4 $\hat{y}^2$ ) <sup>0.5</sup>	$\hat{y}_c \approx 0$	$\hat{y}_c = 0.5$
				0.3033	0
Circular	0.25d <sup>2</sup> $\eta(\hat{y})$	$\{\hat{y} - \frac{1}{2} + \frac{8}{3} \frac{[\hat{y}(1-\hat{y})]^{1.5}}{\eta(\hat{y})}\} d$	2d $[\hat{y}(1-\hat{y})]^{0.5}$	$\hat{y}_c \approx 0$	$\hat{y}_c = 1$
				0.3033	0

### 3. ANALYSIS OF THEORETICAL AND EXPERIMENTAL RESULTS

#### a) Rectangular, triangular and exponential channels

In rectangular channels, the proposed method gives the values of 0.7016 and 0.3033 for EDR and K, respectively. According to Table 2, the values of EDR reported by other investigators have a slight difference (1% to 2%) with the proposed method. The differences between the other formulas with the proposed method are about -1.5% to 3%. In triangular channels, the values of EDR and K by the proposed method are 0.8051 and 0.3558, respectively. Here, all experiments and methods confirm the proposed method. Anderson's method is an exception. In exponential channels, the proposed method gives EDR and K equal to 0.7641 and 0.3366, respectively. This value of EDR has about a 1% to 4% difference with the experimental results reported by other researchers. The differences between the proposed flow discharge with the experimental results are from -4.5% to 2%; Anderson's method gives a difference of about -7.5%.

#### b) Trapezoidal channel

Figure 2a illustrates the variation of EDR with  $my_c/b$  for the trapezoidal channels. It is shown that the experimental results of Diskin [3] and Pagliara and Viti [25] confirm the proposed method, but the experimental data of Keller and Fong [26] have some differences with the results of the presented theory. In addition, the theoretical approach given in this paper is in good agreement with the theoretical approaches of Murty Bhallamudi [11]. Ali and Sykes's [9] theory, in which the free vortex theorem has been used, has some differences with the proposed method.

Table 2. Comparison between the EDR and flow discharge by the proposed model and experimental results of other investigators in rectangular, triangular, and exponential channels

Cross section	Investigator (s)	EDR= $y_b/y_c$	% Difference	Flow discharge (Q)	% Difference	Remark
Rectangular	This study	0.7016	-	$1.7016g^{0.5}by_b^{1.5}$	-	U
	Rouse [1]	0.715	-1.87	$1.654g^{0.5}by_b^{1.5}$	2.88	C
	Rajaratnam & Muralidhar [5]	0.715	-1.87	$1.654g^{0.5}by_b^{1.5}$	2.88	C
		0.705	-0.48	$1.6893g^{0.5}by_b^{1.5}$	0.73	U
	Hager [10]	0.696	0.80	$1.7222g^{0.5}by_b^{1.5}$	-1.20	U
	Murty [11]	0.705	-0.48	$1.6893g^{0.5}by_b^{1.5}$	0.73	U
	Anderson [24]	0.694	1.10	$1.7297g^{0.5}by_b^{1.5}$	-1.62	U
Triangular	This study	0.8051	-	$1.2158g^{0.5}my_b^{2.5}$	-	U
	Rajaratnam & Muralidhar [5]	0.795	1.27	$1.2548g^{0.5}my_b^{2.5}$	-3.11	U
	Ali & Sykes [9]	0.798	0.89	$1.243g^{0.5}my_b^{2.5}$	-2.19	U
	Murty [11]	0.795	1.27	$1.2548g^{0.5}my_b^{2.5}$	-3.11	U
	Ahmad [14]	0.802	0.39	$1.2276g^{0.5}my_b^{2.5}$	-0.96	U
	Anderson [24]	0.762	5.66	$1.395g^{0.5}my_b^{2.5}$	-12.85	U
Exponential	This study	0.7642	-	$\frac{1.7123g^{0.5}c_1y_b^{1.5+c_2}}{(1+c_2)^{1.5}}$	-	U
	Rajaratnam & Muralidhar [5]	0.772	-1.01	$\frac{1.6779g^{0.5}c_1y_b^{1.5+c_2}}{(1+c_2)^{1.5}}$	2.05	U
	Ali & Sykes [9]	0.747	2.30	$\frac{1.7921g^{0.5}c_1y_b^{1.5+c_2}}{(1+c_2)^{1.5}}$	-4.45	U
	Murty [11]	0.758	0.82	$\frac{1.7405g^{0.5}c_1y_b^{1.5+c_2}}{(1+c_2)^{1.5}}$	-1.62	U
	Anderson [24]	0.735	3.97	$\frac{1.8511g^{0.5}c_1y_b^{1.5+c_2}}{(1+c_2)^{1.5}}$	-7.50	U

U= unconfined and C= confined

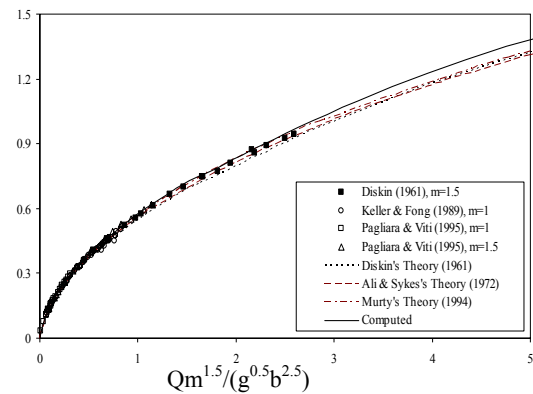
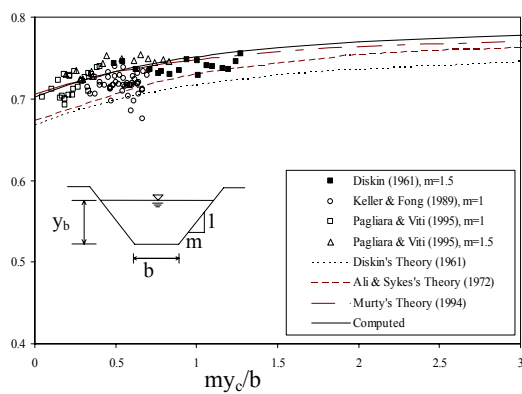


Fig. 2. a) Variation of EDR =  $y_b/y_c$  with  $N_c = m y_c/b$

b) Variation of  $N_b = m y_b/b$  with  $Q m^{1.5}/(g^{0.5} b^{2.5})$  in trapezoidal channels

Figure 2b illustrates the variation of  $m y_b/b$  with  $Q m^{1.5}/(g^{0.5} b^{2.5})$ . From this figure, it can be seen that the

experimental data of Diskin [3], Pagliara and Viti [25], Keller and Fong [26], and also the theoretical approaches of Ali and Sykes [9], and Murty Bhallamudi [11] are in good agreement with the proposed method. In trapezoidal channels, the coefficient of pressure distribution ( $K$ ) changes from 0.3033 for rectangular channels to 0.3558 for triangular channels.

### c) Inverted triangular channel

For inverted triangular channels, the dependence of EDR on  $y_c/z$  is shown in Fig. 3a. Up to  $y_c/z=0.60$ , the EDR varies almost linearly from 0.701 to 0.686. The curve rises sharply from  $y_c/z=0.80$ . The values of EDR from the proposed method are close to the experimental data of Dey and Ravi Kumar [18] with an accuracy of  $\pm 5\%$ . The variation of  $y_b/z$  with  $Q/(g^{0.5}z^{2.5})$  is presented in Fig. 3b. The experimental data of Dey and Ravi Kumar [18] are agreeable with the proposed method with an accuracy of  $\pm 5\%$ . In addition, the computed curve agrees well with their theory. The pressure distribution coefficient ( $K$ ) is equal to 0.3033 for  $y_c/z \approx 0$  (same as a rectangular channel), but is equal to zero for  $y_c/z=1$ .

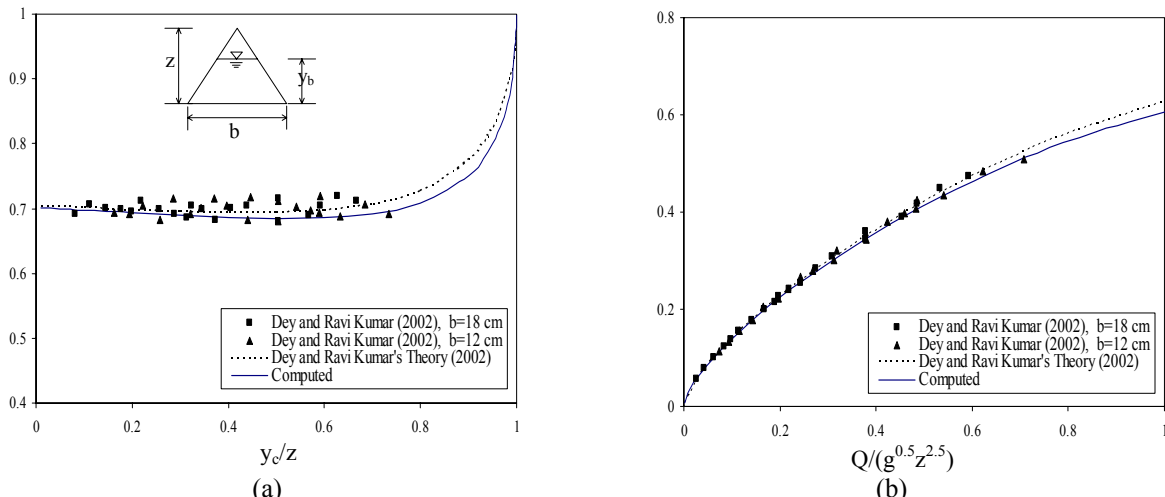


Fig. 3. a) Variation of  $EDR=y_b/y_c$  with  $y_c/z$ ,

b) Variation of  $y_b/z$  with  $Q/(g^{0.5}z^{2.5})$  in inverted triangular channels

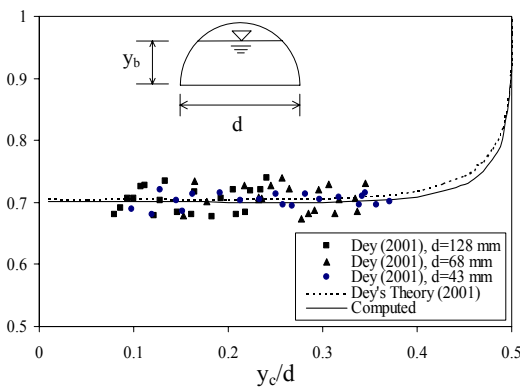
### d) Inverted semicircular channel

The dependence of EDR on  $y_c/d$  is shown in Figure 4a. Up to  $y_c/d=0.40$ , the EDR has a value of about 0.7. The results from the present study agree satisfactorily with the experimental data of Dey [20]. Also, the computed curve agrees well with Dey's theory. Equation (8) in Sterling & Knight's work [13] gives the  $EDR=0.75$ , which slightly overestimates the EDR from the proposed method. Figure 4b can be used to estimate the flow discharge from the measured end-depth. The values of  $K$  are between 0.3033 and zero in the range of  $0 < y_c/d < 0.5$ , which are the same as in inverted triangular channels.

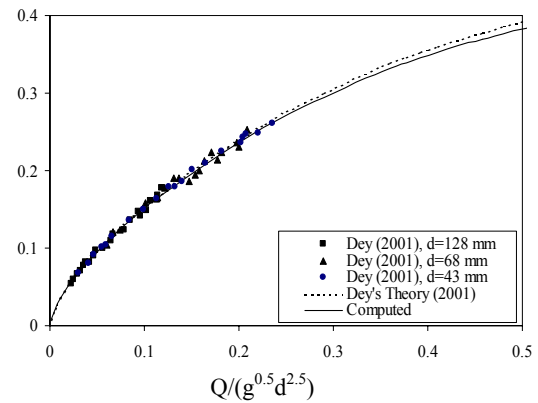
### d) Circular channel

The variation of EDR with  $y_c/d$  is shown in Fig. 5a. In the range of  $0.10 < y_c/d < 0.82$ , the curve obtained from the model lies a little above the experimental data of Rajaratnam and Muralidhar [6]. It is in good agreement with the data of Sterling and Knight [13] and agrees fairly well with the data of Smith [4]. The mean value of the EDR estimated from the experimental data of Smith, Rajaratnam & Muralidhar and also Sterling & Knight are 0.772, 0.725 and 0.743, respectively. The proposed model gives the mean value of EDR around 0.756 in the range of  $0 < y_c/d < 0.7$ . This result is within  $-2\%$ ,  $+4\%$  and  $+2\%$  of the mean value of EDR observed by Smith, Rajaratnam & Muralidhar and Sterling & Knight, respectively. The

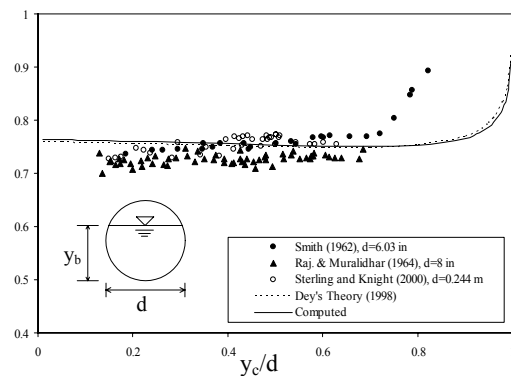
computed curve agrees very well with Dey's theory [15]. The variation of  $y_b/d$  with  $Q/(g^{0.5}d^{2.5})$  is shown in Fig. 5b. The experimental data of Smith, Rajaratnam and Muralidhar and also Sterling and Knight agree well with the obtained curve for  $Q/(g^{0.5}d^{2.5}) < 0.50$ . However, the experimental data of Smith for large values of  $Q/(g^{0.5}d^{2.5})$  are underestimated by the proposed method. In addition, the computed curve agrees well with Dey's theory [15]. The pressure coefficient (K) is equal to 0.3366 for  $y_c/d \approx 0$  (same as an exponential channel), and decreases when critical depth  $y_c$  increases and reaches zero for  $y_c/d = 1$ .



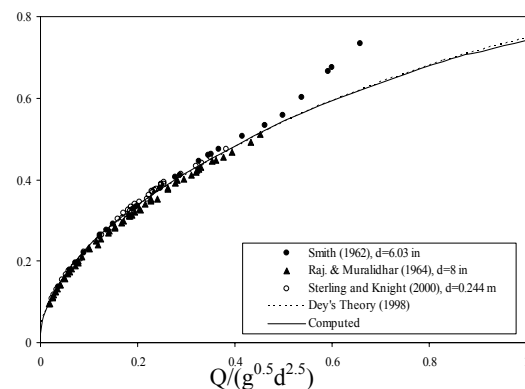
(a)

Fig. 4. a) Variation of EDR= $y_b/y_c$  with  $y_c/d$ 

(b)

b) Variation of  $y_b/d$  with  $Q/(g^{0.5}d^{2.5})$  in inverted semicircular channels

(a)

Fig. 5. a) Variation of EDR= $y_b/y_c$  with  $y_c/d$ 

(b)

b) Variation of  $y_b/d$  with  $Q/(g^{0.5}d^{2.5})$  in circular channels

Fig. 5a shows that at low depths of flow, the proposed method and also Dey's theory are unable to give the proper results. Based on experiments, Sterling & Knight [13] gave an interesting hypothesis that the hydraulic behavior of a circular channel at low flow depths is similar to a trapezoidal channel and none of the theories that account for the variation of the EDR can be successfully applied to a circular channel. Experimental data on Fig. 2a and Fig. 5a confirm their idea. It can be added that the hydraulic behavior of an inverted semicircular channel for the variation of EDR with  $y_c/d$  (Fig. 4a) is the same as that of an inverted triangular channel (Fig. 3a). In this case, both the proposed and Dey's theories can be successfully used in these channels.

(b)

The existence of abrupt discontinuity in the EDR at  $y_c/d > 0.73$  and discharge relationship at  $Q/(g^{0.5}d^{2.5}) > 0.50$  for the experimental data of Smith [4] in Fig. 5 needs further clarification. In a circular channel, when  $y_n/d$  is greater than 0.82 ( $y_n$  is the uniform flow depth), it is possible to have two different

depths for the same discharge [22, 24]. Since in a mildly sloping channel the critical depth is less than the uniform flow depth, one can expect that for some lower depths where  $y_c/d$  is a bit less than 0.82, the conduit simply flow full. Under these conditions, cross-waves in the water surface can exist and accurate measurements of the flow is practically impossible. In addition, Smith [4] indicated that the exact point at which the discontinuity occurs varies with the channel slope. A steeper slope can delay the discontinuity to a value  $y_c/d$  greater than 0.73 or  $Q/(g^{0.5}d^{2.5}) > 0.50$ . It seems that a similar condition might occur in any gradually closing conduit. Additional tests are required to establish the correct discharge relationship in these channels.

#### 4. CONCLUSIONS

Based on the free vortex theorem the pressure distributions at the brink depth and end-pressure coefficient (K) of the free overfall in horizontal or mildly sloping channels with different cross sections have been theoretically estimated. Using the momentum equation, the end depth ratio (EDR) is obtained. For design purposes, charts have been constructed to facilitate the prediction of flow discharge when EDR is known. The proposed method has been verified with the available experimental and theoretical results of other investigators. The results showed that:

-The EDR in rectangular, triangular, and exponential channels are 0.7016, 0.8051, and 0.7642, respectively. The proposed model is valid in trapezoidal channels with  $my_b/b < 1$ , in inverted triangular with  $y_b/z < 0.5$ , in inverted semicircular with  $y_b/d < 0.3$ , and in circular channels with  $y_b/d < 0.5$  within  $\pm 5\%$  error with the experimental results and agrees very well with the theoretical approaches of other investigators.

-The presented theory, as well as some complicated theories of other investigators (e.g., 15, 18, 20) give almost the same results. In addition, the proposed theory is capable of predicting the pressure distribution of the brink section.

-None of the existing theories which account for the determination of EDR can be successfully applied to a circular channel. A circular channel at low flow depths resembles a trapezoidal channel. The hydraulic behavior of an inverted semicircular channel is similar to an inverted triangular channel.

-The writers believe that the presented method can also be used for the super-critical approaching flow. In the latter case, using Manning's equation and the control volume between the end-depth and uniform flow depth, flow discharge as a function of the end-depth and channel slope can be easily estimated.

#### REFERENCES

1. Rouse, H. (1936). Discharge characteristics of the free overfall. *Civ. Eng., ASCE*, 6(4), 257–260.
2. Dey, S. (2002). Free overfall in open channels: State-of-the-art review. *Flow Meas. Instrum.*, 13, 247–264.
3. Diskin, M. H. (1961). The end depth at a drop in trapezoidal channels. *J. Hydr. Div., ASCE*, 87(4), 11–32.
4. Smith, C. D. (1962). Brink depth for a circular channel. *J. Hydr. Div., ASCE*, 88(6), 125–134.
5. Rajaratnam, N. & Muralidhar, D. (1964). End depth for exponential channels. *J. Irrig. & Drain. Eng., ASCE*, 90(1), 17–36.
6. Rajaratnam, N. & Muralidhar, D. (1964). End depth for circular channels. *J. Hydr. Div., ASCE*, 90(2), 99–119.
7. Rajaratnam, N. & Muralidhar, D. (1968). Characteristics of rectangular free overfall. *J. Hydr. Res.*, 6(3), 233–258.
8. Rajaratnam, N. & Muralidhar, D. (1970). The trapezoidal free overfall. *J. Hydr. Res.*, 8(4), 419–447.
9. Ali, K. H. M. & Sykes, A. (1972). Free-vortex theory applied to free overfall. *J. Hydr. Div., ASCE*, 98(5), 973–979.
10. Hager, W. H. (1983). Hydraulics of the plane overfall. *J. Hydr. Eng., ASCE*, 109(2), 1683–1697.

11. Murty Bhallamudi, S. (1994). End depth in trapezoidal and exponential channels. *J. Hydr. Res.*, 32(2), 219–232.
12. Ferro, V. (1999). Theoretical end-depth-discharge relationships for free overfall. *J. Irrig. & Drain. Eng., ASCE*, 125(1), 40–44.
13. Sterling, M. & Knight, D. W. (2001). The free overfall as a flow-measuring device in a circular channel. *Proc. Inst. Civ. Eng., Waters Maritime Energ.*, 148(Dec.), 235–243.
14. Ahmad, Z. (2002). Free overfall as measuring device in triangular channels. *Conf. of Hydr., Water Resour. And Ocean Eng.*, 115–119.
15. Dey, S. (1998). End depth in circular channels. *J. Hydr. Eng., ASCE*, 124(8), 856–863.
16. Dey, S. (2001). EDR in circular channels. *J. Irrig. Drain. Eng., ASCE*, 127(2), 110–112.
17. Dey, S. (2001). Flow metering by end-depth method in elliptic channels. *Dam Eng.*, 12(1), 5–19.
18. Dey, S. & Ravi Kumar, B. (2002). Hydraulics of free overfall in  $\Delta$  shaped channels. *Sadhana Proc. Indian Acad. Sci.*, 27(June), 353-363.
19. Dey, S. (2002). Free overfall in circular channels with flat base: A method of open channel flow measurement. *Flow Meas. and Instrum.*, 13, 209-221.
20. Dey, S. (2003). Free overfall in inverted semicircular channels. *J. Hydr. Eng., ASCE*, 129(6), 438–447.
21. Dey, S. (2003). Overfall in U-Shaped Channels. *J. Mech. Eng., ASCE*, 129(3), 358–362.
22. Chow, V. T. (1959). *Open channel hydraulics*. McGraw Hill Publishing Company, New York.
23. Henderson, F. M. (1966). *Open Channel Flow*. Macmillan Book Company.
24. Subramanya, K. (1987). *Flow in open channels*. Tata McGraw Hill Publishing Company, New Delhi.
25. Pagliara, S. & Viti, C. (1995). Discussion on Gupta, R. D., Jamil, M. & Mohsin, M. 1993. *J. Irrig. & Drain. Eng., ASCE*, 121(1), 128–130.
26. Keller, R. J. & Fong, S. S. (1989). Flow measurement with trapezoidal free overfall. *J. Irrig. & Drain. Eng., ASCE*, 115(1), 125–136.